Molecular Pharmacology Fast Forward. Published on January 21, 2019 as DOI: 10.1124/mol.118.114751
This article has not been copyedited and formatted. The final version may differ from this version.

Blockade of the human ether a-go-go related gene (hERG) potassium channel by fentanyl

Jared N. Tschirhart, Wentao Li, Jun Guo, and Shetuan Zhang

Department of Biomedical and Molecular Sciences, Queen's University, Kingston, Ontario, Canada

Molecular Pharmacology Fast Forward. Published on January 21, 2019 as DOI: 10.1124/mol.118.114751
This article has not been copyedited and formatted. The final version may differ from this version.

Running Title: Fentanyl-mediated block of hERG channels

Address correspondence to:

Dr. Shetuan Zhang, Department of Biomedical and Molecular Sciences, Queen's University, 18 Stuart Street, Kingston, Ontario, K7L 3N6 Canada. Tel: (613) 533-3348; Fax: (613) 533-6412; E-mail: shetuan.zhang@queensu.ca

Manuscript information:

Text pages: 22

Tables: 0

Figures: 10

References: 52

Abstract: 244

Introduction: 482

Discussion: 1667

Abbreviations: AP, action potential; APD_{90}, action potential duration at 90% repolarization; EAG, ether-a-go-go; HEK, human embryonic kidney; hERG, human ether a-go-go related gene; IC_{50}, half maximal inhibitory concentration; ICA, ICA-105574, 3-nitro-N-(4-phenoxyphenyl)-benzamide; I_{Ca}, calcium current; I_{hERG}, hERG current; I_K, potassium current; I_{Kr}, rapidly activating delayed rectifier potassium current; I_{Na}, sodium current; LQTS, long QT syndrome; MEM, minimum essential medium; PBS, phosphate buffered saline; QTc, corrected QT interval; τ_{inact}, time constant of inactivation; τ_{recv}, time constant of recovery from inactivation; $\tau_{f\text{-}deact}$, fast time constant of deactivation; $\tau_{s\text{-}deact}$, slow time constant of deactivation; $V_{1/2}$, voltage of half maximal activation.

Molecular Pharmacology Fast Forward. Published on January 21, 2019 as DOI: 10.1124/mol.118.114751
This article has not been copyedited and formatted. The final version may differ from this version.

ABSTRACT

The *human ether-a-go-go-related gene* (*hERG*) encodes the pore-forming subunit of the rapidly activating delayed rectifier potassium channel (I_{Kr}). Drug- or medical condition-mediated disruption of hERG function is the primary cause of acquired long QT syndrome (LQTS), which predisposes affected individuals to ventricular arrhythmias and sudden death. Fentanyl abuse poses a serious health concern, with abuse and death rates rising over recent years. As fentanyl has a propensity to cause sudden death, we investigated its effects on the hERG channel. The effects of norfentanyl, the main metabolite, and naloxone, an antidote used in fentanyl overdose, were also examined. Currents of hERG channels stably expressed in HEK293 cells were recorded using whole-cell voltage-clamp method. When hERG tail currents upon −50 mV repolarization following a 50 mV depolarization were analyzed, fentanyl and naloxone blocked hERG current (I_{hERG}) with an IC_{50} of 0.9 μM and 74.3 μM, respectively, while norfentanyl did not block. However, fentanyl-mediated block of I_{hERG} was voltage-dependent. When a voltage protocol that mimics a human ventricular action potential (AP) was used, fentanyl blocked I_{hERG} with an IC_{50} of 0.3 μM. Furthermore, fentanyl (0.5 μM) prolonged AP duration and blocked I_{Kr} in ventricular myocytes isolated from neonatal rats. The concentrations of fentanyl used in this study were higher than seen with clinical use but overlap with post-mortem overdose concentrations. While mechanisms of fentanyl-related sudden death need further investigation, blockade of hERG channels may contribute to the death of individuals with high-concentration overdose or compromised cardiac repolarization.

Molecular Pharmacology Fast Forward. Published on January 21, 2019 as DOI: 10.1124/mol.118.114751
This article has not been copyedited and formatted. The final version may differ from this version.

INTRODUCTION

The *human ether-a-go-go related gene* (*hERG*) encodes the pore-forming subunit of the rapidly activating delayed rectifier potassium channel (I_{Kr}) (Sanguinetti *et al.*, 1995; Trudeau *et al.*, 1995), which is critical for repolarization of the cardiac action potential (AP) (Keating and Sanguinetti, 2001; Curran *et al.*, 1995). A decrease in hERG channel function causes long QT syndrome (LQTS), predisposing affected individuals to Torsade de Pointes ventricular arrhythmia and sudden cardiac death (Keating and Sanguinetti, 2001). While the function of hERG channels can be impaired by naturally occurring mutations (Zhou *et al.*, 1998a), it is more often compromised by various compounds including certain medications (Zhou *et al.*, 1999; Zhang *et al.*, 1999). Although activities of various channels contribute to the formation of cardiac APs, the block of hERG by drugs is a common mechanism for acquired LQTS (Fenichel *et al.*, 2004).

In recent years, fentanyl-associated death has become a serious issue in North America. Fentanyl is a potent synthetic opioid that acts as a μ-opioid receptor agonist (Raynor *et al.*, 1994). It is used clinically for pain management and anesthesia but is also used illicitly (Stanley, 2014). Fentanyl use poses a risk due to its addictive characteristics and side-effects, particularly its propensity to cause sudden death. It is known that fentanyl reduces chemosensitivity, causing respiratory depression (Santiago and Edelman, 1985). However, it is unclear whether cardiac arrhythmias also play a role in fentanyl-related deaths. While synthetic opioids such as methadone (Kornick *et al.*, 2003; Krantz *et al.*, 2003; Maremmani *et al.*, 2005; Martell *et al.*, 2005) have been observed to prolong the QT interval in humans, the clinical literature regarding fentanyl is less clear; both unchanged and prolonged QT intervals have been reported (Cafiero *et al.*, 2011; Keller *et al.*, 2016). Experimentally, fentanyl at concentrations of 94.6 nM, 0.19 μM,

and 0.95 μM prolongs the cardiac AP in isolated canine ventricular Purkinje fibers (Blair *et al.*, 1989). Since the prolongation is not reversed by naloxone, it likely arises from a mechanism separate from μ-opioid receptor agonism (Blair *et al.*, 1989). Since reduction of I_{Kr} prolongs AP duration and is responsible for most cases of drug-induced LQTS, we investigated the effects of fentanyl on hERG channels stably expressed in a hERG-HEK cell line. We also examined the effects of fentanyl on cardiac APs and various currents in neonatal rat ventricular myocytes. Furthermore, the effects of norfentanyl, the physiologic metabolite of fentanyl (Labroo *et al.*, 1997), as well as naloxone, an antidote for fentanyl overdose (Wang *et al.*, 2007), were studied. Our data showed that norfentanyl did not block I_{hERG} and naloxone only blocked I_{hERG} at tens to hundreds micromolar concentrations. However, submicromolar concentrations of fentanyl blocked I_{hERG}, which could not be reversed by naloxone. Our data further revealed that fentanyl-mediated block of I_{hERG} was strongly voltage-dependent, but was independent of channel inactivation gating. Fentanyl also blocked I_{Kr} and prolonged APs in neonatal rat ventricular myocytes.

MATERIALS AND METHODS

Molecular Biology

hERG cDNA was provided by Dr. Gail Robertson (University of Wisconsin-Madison). Point mutations Y652A, F656T, S631A, S620T, and S620C were created using PCR overlap extension technique as described previously (Guo *et al.*, 2006). Human EAG cDNA was provided by Dr. Luis Pardo (Max-Planck Institute of Experimental Medicine, Göttingen, Germany). Human Kv1.5 cDNA was provided by Dr. Michael Tamkun (Colorado State University, Fort Collins, Colorado). Human KCNQ1 and KCNE1 cDNAs were provided by Dr.

Michael Sanguinetti (University of Utah). Human Kv4.3 was provided by Gui-Rong Li (University of Hong Kong). Human Kir2.3 cDNA was provided by Dr. Carol Vandenberg (University of California, Santa Barbara). The HEK293 cell line stably expressing WT hERG channels (hERG-HEK cell line) was obtained from Dr. Craig January (University of Wisconsin, Madison). HEK293 cell lines stably expressing EAG, Kv1.5, and KCNQ1+KCNE1 were created using transfection followed by G418 selection. Kv4.3, Kir2.3 and mutant hERG Y652A, F656T, S631A, S620C, and S620T were transiently expressed in HEK293 cells. For transient transfection, GFP cDNA (pIRES2-EGFP, Clontech, CA) was cotransfected for selection of transfected cells during patch clamp experiments. HEK 293 cells were cultured in Gibco Minimum Essential Medium (MEM) supplemented with 10% fetal bovine serum, nonessential amino acids, and 1 mM sodium pyruvate (Thermo Fisher Scientific). For electrophysiological recordings, the cells were collected from the culture dish using trypsinization and kept in MEM at room temperature until used (within 4 h).

Neonatal rat ventricular myocyte isolation

Neonatal rat experiments were approved by the Queen's University Animal Care Committee and performed in conformity with the Canadian Council on Animal Care. Sprague-Dawley rats of either sex were used for isolation of ventricular myocytes at one day of age. Neonatal rats were sacrificed by rapid decapitation with scissors followed by heart removal using scissors and forceps. Hearts were then washed twice with filtered phosphate buffered saline (PBS) on ice and minced with scissors. The minced hearts were washed twice with ice cold PBS, and then incubated with 8.5 mL PBS, 500 μL collagenase (740 U), 500 μL trypsin (370 U), and 500 μL DNAse (2880 U) at 37°C for 10 min to dissociate single ventricular myocytes. The supernatant was then extracted

and placed in 20 mL of 20% FBS in DF medium (Dulbecco's modified eagle medium/F12 supplemented with 3 mM $NaHCO_3$, 15 mM HEPES, and 50 mg/mL gentamycin). The enzymatic digestion and extraction were repeated 6 times. On the last three digestions, the minced hearts were gently aspirated with a pipette to maximize the dissociation of cells. The cell mixture was then centrifuged at 95×g for 5 min. The supernatant was discarded. The viable cardiomyocytes were then extracted by Percoll density separation. Specifically, Percoll (GE Healthcare, Little Chalfont, UK) was diluted in appropriate amounts of Ads buffer (6.8 g NaCl, 1.0 g dextrose, 1.5 g NaH_2PO_4, 0.4 g KCl, 0.1 g $MgSO_4$, 4.76 g HEPES in 1 L double-distilled water) to create 10 mL of three separate densities: 1.050 g/mL, 1.060 g/mL, and 1.082 g/mL. Phenol red was added to the 1.060 g/mL solution to allow for distinction between the layers. First, 10 mL of the 1.050 g/mL solution was added to a new centrifuge tube. Next, 10 mL of 1.060 g/mL solution was carefully added below using a pipette. Lastly, the cell pellet was resuspended in 10 mL of 1.082 g/mL solution and carefully added below the 1.060 g/mL layer. The tube was then centrifuged at room temperature (22±1°C) for 30 min at 483×g (with the brake disabled to avoid disrupting the gradient). The layer containing the cardiomyocytes (at the bottom of the red phase, between the 1.060 g/mL and 1.082 g/mL phases) was carefully removed with a micropipette, mixed in 45 mL 10% FBS containing DF, and centrifuged for 5 min at 95×g. The pellet containing cardiomyocytes was then resuspended in 20 mL of 10% FBS-containing DF medium and pre-plated on 100 mm plates. The plates were incubated at 37 °C with 5% CO_2 for 45 min to allow fibroblasts to adhere to the bottom of the plate. The media (containing cardiomyocytes) was then transferred to culture plates with glass coverslips and cultured overnight (16 h) in 10% FBS in DF medium before electrophysiological recording.

Molecular Pharmacology Fast Forward. Published on January 21, 2019 as DOI: 10.1124/mol.118.114751
This article has not been copyedited and formatted. The final version may differ from this version.

Western blot analysis

After 16-h culture in media containing 10 μM of the respective drugs, hERG-HEK cells were collected with ice-cold phosphate-buffered saline (PBS). Cells were lysed by sonication in ice-cold radioimmunoprecipitation assay lysis buffer supplemented with 1% phenylmethylsulfonyl fluoride and 2% protease inhibitor cocktail. A DC Protein Assay Kit (Bio-Rad, Hercules, CA) was used to determine protein concentration of samples. 15 μg of protein sample was diluted to a volume of 40 μL with double-distilled water. The 40 μl sample was resuspended in 10 μL of 5 × Laemmli loading buffer containing 5% β-mercaptoethanol to achieve a total volume of 50 μL, and boiled for 5 min. The 50 μL samples were separated on 8% SDS polyacrylamide electrophoresis gels and transferred overnight onto polyvinylidene difluoride membranes. The membranes were blocked for 1 h using 5% non-fat milk. The blots were probed for 2 h with the appropriate primary antibodies in 5% non-fat milk and then incubated with the corresponding horseradish peroxidase (HRP)-conjugated secondary antibodies in 5% non-fat milk for an additional hour. Primary and secondary antibody incubations were followed by triple 10-min washes in Tris-Buffered Saline and Tween 20 (TBST, 0.1% Tween-20). Detection of actin was used as loading control. The blots were visualized with Fuji medical X-ray films (Minato, Tokyo, Japan) using an enhanced chemiluminescence detection kit (GE Healthcare, Little Chalfont, United Kingdom). Densitometry analyses of protein band intensities were performed using ImageJ. Band sizes were identified using BLUeye Prestained protein ladder (GeneDirex, Taiwan) loaded on each gel. For quantification, the band intensities of proteins of interest in each gel were first normalized to their respective actin (loading control) intensities and then expressed as values relative to the control.

Molecular Pharmacology Fast Forward. Published on January 21, 2019 as DOI: 10.1124/mol.118.114751
This article has not been copyedited and formatted. The final version may differ from this version.

Electrophysiological recordings

The whole-cell voltage-clamp method was used to record various currents in HEK cells and isolated neonatal rat ventricular myocytes. Whole-cell current clamp was used to record APs from isolated neonatal rat ventricular myocytes. Pipettes were pulled from thin-walled borosilicate glass (World Precision Instruments, Sarasota, CA) with a P-1000 micropipette puller (Sutter Instrument, Novato, CA) and polished with heat to a resistance of ~2.0 MΩ when filled with solution. An Axopatch 200B amplifier, Digidata 1440A digitizer, and pCLAMP10.7 software (Molecular Devices, San Jose, CA) were used for data acquisition and analysis. The pipette solution for recording from channels expressed in HEK cells, as well as I_K and APs from isolated neonatal rat ventricular myocytes contained (in mM) 135 KCl, 5 EGTA, 5 MgATP, and 10 HEPES (pH 7.2 with KOH). The bath solution contained (in mM) 5 KCl, 135 NaCl, 2 $CaCl_2$, 1 $MgCl_2$, 10 glucose, and 10 HEPES (pH 7.4 with NaOH). To record I_{Na} and I_{Ca}, the pipette solution consisted of (in mM) 135 CsCl, 10 EGTA, 5 MgATP, and 10 HEPES (pH 7.2 with CsOH). For recording I_{Na}, the bath solution consisted of (in mM) 100 TEACl, 40 NaCl, 5 KCl, 1 $MgCl_2$, 10 glucose, and 10 HEPES (pH 7.4 with TEAOH). To record Ba^{2+}-mediated I_{Ca} ($I_{Ca\text{-}Ba}$), the bath solution consisted of (in mM) 140 TEACl, 5.4 $BaCl_2$, 1 $MgCl_2$, 10 glucose, and 10 HEPES (pH 7.4 with TEAOH). Recordings were carried out at room temperature (22±1°C).

Drugs and reagents

Fentanyl citrate, norfentanyl hydrochloride, and naloxone hydrochloride were purchased from Toronto Research Chemicals (North York, ON). Drugs were dissolved in double-distilled water and stored at −20°C. For patch-clamp experiments, the drugs were diluted in bath solution and used within 8 h. MEM, FBS, G418 (Geneticin), non-essential amino acids, and sodium

pyruvate were purchased from Thermo Fisher Scientific (Waltham, MA). E-4031 dihydrochloride was purchased from Tocris Bioscience (Bristol, United Kingdom), dissolved in double-distilled water stored at −20°C, and diluted in bath solution for patch clamp experiments. Mouse anti-actin primary antibody, ICA-105574, electrolytes, EGTA, HEPES, glucose, and BSA were purchased from Sigma-Aldrich (St. Louis, MO). Goat anti-hERG (C-20) primary antibody, and mouse anti-goat HRP-conjugated secondary antibody were purchased from Santa Cruz Biotechnology (Dallas, TX). Horse anti-mouse HRP-conjugated secondary antibody was purchased from Cell Signaling Technology (Danvers, MA). The C-20 primary antibody was used in a 1:1000 dilution, anti-actin primary antibody was used in a 1:2000 dilution, and anti-mouse and anti-goat HRP-conjugated secondary antibodies were used in a 1:20000 dilution.

Statistical analysis

All data are expressed as the mean ± standard deviation (SD). A one-way ANOVA with Tukey post-hoc test or 2-tailed Student's *t*-test were used to determine statistical significance between the control and test groups. For normalized data, a Wilcoxon matched pairs test was used to compare currents with fentanyl to control currents at each voltage. Statistical analysis was performed with GraphPad Prism. A *P*-value of 0.05 or less was considered statistically significant.

RESULTS

Fentanyl, but neither norfentanyl nor naloxone, appreciably block hERG currents

Whole-cell voltage-clamp technique was used to record I_{hERG} from hERG-HEK cells before and after drug application to the bath solution. I_{hERG} was elicited with the voltage protocol

Molecular Pharmacology Fast Forward. Published on January 21, 2019 as DOI: 10.1124/mol.118.114751
This article has not been copyedited and formatted. The final version may differ from this version.

shown above the current traces at a pulse interval of 15 s. Due to the characteristic rapid inactivation properties (Spector *et al.*, 1996b), hERG channels activate and inactivate during the depolarizing step. Upon the repolarizing step, inactivated hERG channels rapidly recover to the open state and then slowly deactivate. This leads to the characteristic tail current, which represents maximal channel conductance, and was used to quantify the amplitude of I_{hERG}. Fentanyl blocked I_{hERG} in a concentration-dependent manner (Fig. 1A), and the blocked currents recovered completely within 1 min upon washout. While naloxone at concentrations much higher than clinically relevant doses also blocked I_{hERG}, norfentanyl did not block I_{hERG}. The amplitudes of I_{hERG} relative to control were plotted against corresponding fentanyl, norfentanyl, and naloxone concentrations, and fitted to the Hill equation when appropriate. Fentanyl blocked I_{hERG} with an IC_{50} of 0.9±0.5 μM and a Hill coefficient of 0.9±0.3. Naloxone blocked I_{hERG} with an IC_{50} of 74.3±36.2 μM and a Hill coefficient of 0.9±0.1. Norfentanyl did not affect I_{hERG} at concentrations up to 300 μM (Fig. 1B).

Fentanyl-mediated decrease in I_{hERG} is not reversed by naloxone

To determine whether fentanyl-induced reduction of I_{hERG} can be prevented by naloxone, we applied fentanyl alone, and then fentanyl plus naloxone to the same hERG-HEK cells during patch-clamp recordings. Our results showed that 1 μM of fentanyl reduced I_{hERG} by 50.0±7.8% compared to control. When 1 μM fentanyl and 10 μM naloxone were applied together to the same cells, current was decreased by 58.1±7.6% compared to control (Fig. 1C). Although naloxone caused a slight further decrease in I_{hERG}, this change was not significant. Therefore, naloxone does not reverse the block of hERG channels by fentanyl.

Molecular Pharmacology Fast Forward. Published on January 21, 2019 as DOI: 10.1124/mol.118.114751
This article has not been copyedited and formatted. The final version may differ from this version.

Fentanyl, norfentanyl, and naloxone do not affect hERG membrane expression

To determine the chronic effects of fentanyl, norfentanyl, and naloxone on hERG channel expression, hERG-HEK cells were cultured overnight (16 h) with 10 μM of each compound. Whole-cell protein was then extracted and analyzed using Western blot analysis. Whole-cell hERG proteins display two bands (Zhou *et al.*, 1998b). The lower (135 kDa) band represents the immature, core glycosylated protein located in the endoplasmic reticulum. The upper (155 kDa) band represents the mature fully glycosylated protein located in the plasma membrane. Chronic treatment with 10 μM of fentanyl, norfentanyl, or naloxone did not decrease hERG channel expression (Fig. 1D) or I_{hERG} (data not shown).

Fentanyl-mediated block is specific to hERG

To determine if fentanyl blocks other K^+ channels, we studied the effects of fentanyl on hERG along with other channels including EAG, Kv1.5, KCNQ1+KCNE1, Kv4.3, and Kir2.3 stably or transiently expressed in HEK cells. As shown in Figure 2, acute application of 10 μM fentanyl reduced I_{hERG} by 89.2±7.1% (P<0.01 compared to control) but did not reduce other channel currents studied (P>0.05 compared to control, Fig. 2).

Effects of fentanyl on hERG biophysical properties

The effect of fentanyl on hERG voltage dependence of activation was studied. Figure 3A shows families of hERG currents elicited with the voltage protocol above the current traces in the absence and presence of 1 μM fentanyl. The pulse currents measured at the end of the depolarization steps and the peak tail currents measured during the −50 mV repolarizing step,

Molecular Pharmacology Fast Forward. Published on January 21, 2019 as DOI: 10.1124/mol.118.114751
This article has not been copyedited and formatted. The final version may differ from this version.

normalized to their respective maximal amplitude in control, were plotted versus activation (depolarization) voltages. The tail current - voltage relationships were fitted to the Boltzmann equation. In addition to block, fentanyl shifted the half maximal activation voltage ($V_{1/2}$) to negative voltages by 14.3 mV (−5.7±2.8 mV in control; −20.0±4.3 mV with fentanyl, P<0.01). It also increased the slope factor from 6.6±0.8 in control to 11.2±2.1 (P<0.01). Due to the changes in $V_{1/2}$ and slope factor, an interesting observation is that I_{hERG} with fentanyl is slightly greater at voltages between −20 mV and −50 mV (P<0.01) despite being reduced at 0 mV and above (P<0.01) (Fig. 3A).

We used a three-pulse voltage protocol to study the effects of fentanyl on hERG inactivation. hERG-HEK cells were depolarized to 60 mV for 500 ms to activate and inactivate hERG channels. The cells were then repolarized to −100 mV for 5 ms, allowing inactivated channels to recover to the open state with minimal deactivation (Zhou *et al.*, 1998b). The third step to voltages between −30 and 130 mV in 10 mV increments was used to elicit hERG inactivation. The decay of hERG currents during the third step were fitted to a single exponential function to obtain the time constants of inactivation (τ_{inact}). Fentanyl decreased τ_{inact} at voltages of 0 mV and below (P<0.05) (Fig. 3B).

To study the effects of fentanyl on hERG recovery from inactivation and deactivation, we depolarized cells to 60 mV for 1 s to activate and inactivate the channels. The cells were then stepped to voltages between −160 mV and 30 mV in 10 mV increments to cause channel recovery from inactivation (the rising phase of currents) and deactivation (the decay phase of currents) (Fig. 3C). The rising phase of currents were fitted to single exponential functions to obtain the time constants of recovery from inactivation (τ_{recv}), which were plotted versus the repolarizing voltages. Fentanyl slightly shifted τ_{recv} in the negative direction (Fig. 3C). The decay

Molecular Pharmacology Fast Forward. Published on January 21, 2019 as DOI: 10.1124/mol.118.114751
This article has not been copyedited and formatted. The final version may differ from this version.

phases of currents were fitted to double exponential functions to obtain the time constants of deactivation (τ_{deact}), which were plotted versus the repolarizing voltages (Fig. 3D). For deactivation, only voltages between −90 and −160 mV were analyzed as deactivation was prominent and the current decay could be reliably fitted to determine the fast ($\tau_{f\text{-}deact}$) and slow ($\tau_{s\text{-}deact}$) times constants of deactivation. Fentanyl decreased $\tau_{f\text{-}deact}$ and $\tau_{s\text{-}deact}$ (P<0.05).

Fentanyl blocks hERG in the open state

To investigate if fentanyl blocks hERG in the open state, we depolarized cells to 120 mV for 40 ms to quickly activate the channels followed by 4-s at 0 mV to maintain channel opening. The cells were finally repolarized to –50 mV for 500 ms prior to returning to the holding potential of –80 mV. After recording control current, 2 μM fentanyl was immediately applied during the pulse interval of 60 s when the cell was held at –80 mV. As shown in Figure 4A, fentanyl-mediated block of hERG developed with time when channels were opened despite the drug being present for 1-min prior to the channel opening. The time-dependent block was most obvious upon the first trace after fentanyl application (arrow a). Upon the second and subsequent depolarizing steps (arrow b), the initial current was largely blocked, but a slight development of block during the 0 mV step was still present. These data indicate that fentanyl preferentially blocks open channels, and a very small amount of unblock occurs during the pulse interval when channels are closed at the holding potential of –80 mV.

Open-channel blockers can be trapped by channel closing upon repolarization (Mitcheson *et al.*, 2000b; Stork *et al.*, 2007; Witchel *et al.*, 2004). To investigate whether fentanyl can be trapped by hERG channel closing, we first achieved steady-state of channel block by recording hERG currents using the voltage protocol shown in the top of Figure 4 for 5 min with 2 μM

fentanyl present in the bath solution. We then completely washed out fentanyl (within 2 s) while cells were held at –80 mV for 60 s to maintain closed channel state before applying the next depolarizing sweep to elicit hERG currents. As shown in Figure 4B, when the channels were opened, the current gradually recovered (arrow a) to control level within the 4-s sweep. After the first trace of washout, current remains at control levels (arrow b). Thus, fentanyl is trapped by hERG channel closure, and is only released upon channel opening.

Fentanyl shares a binding site with other typical hERG blocking drugs

To characterize the binding site of fentanyl, we examined its competition with E-4031 (N-[4-[1-[2-(6-methylpyridin-2-yl)ethyl]piperidine-4-carbonyl]phenyl]methanesulfonamide), a well-studied hERG blocking drug (Sanguinetti and Jurkiewicz, 1990; Spector *et al.*, 1996a; Trudeau *et al.*, 1995). When I_{hERG} was recorded by repetitive pulsing to 50 mV for 4 s followed by –50 mV for 5 s at a pulse-interval of 15 s, 10 μM fentanyl-mediated block was achieved after the first pulse during 15-min recordings. Upon washout of fentanyl, I_{hERG} quickly recovered to 85.0±18.9% of control (n=4) (Fig. 5A, left). However, recovery of I_{hERG} after 0.5 μM E-4031 block is minimal and slow, to 10.1±4.1% of control (n=4) after 10 min washout (Fig. 5A, middle). To determine if fentanyl and E-4031 compete for a common binding site on hERG, 10 μM fentanyl was applied to block the channel while additional 0.5 μM E-4031 was applied in the same manner as when it was applied alone (Fig. 5A, right). Upon washout of E-4031 and subsequently fentanyl, I_{hERG} recovered more than that from E-4031 block alone, to 43.2±16.2% (n=7, $P<0.01$ versus E-4031 alone). These data suggest that fentanyl may share binding site(s) with E-4031 to block hERG channels.

Molecular Pharmacology Fast Forward. Published on January 21, 2019 as DOI: 10.1124/mol.118.114751
This article has not been copyedited and formatted. The final version may differ from this version.

High-affinity binding of E-4031 and many other hERG blockers involves Tyr652 and Phe656 of the S6 transmembrane segment (Lees-Miller *et al.*, 2000; Mitcheson *et al.*, 2000a; Perry *et al.*, 2004; Guo *et al.*, 2006). Therefore, we examined fentanyl block in Y652A and F656T mutant hERG channels. Y652A and F656T were resistant to block by 10 μM fentanyl (P<0.01 versus WT) (Fig. 5B), supporting the notion that fentanyl interacts with the typical hERG binding site involving residues Tyr652 and Phe656.

hERG inactivation is not required for fentanyl block

In addition to a common binding site, inactivation gating plays a critical role in high-affinity binding of various compounds to hERG channels (Wang *et al.*, 1997; Ficker *et al.*, 1998; Zhang *et al.*, 1999; Chen *et al.*, 2002). We examined whether fentanyl-mediated hERG block is also dependent on channel inactivation. To this end, we used three hERG inactivation mutants, S631A, S620T, and S620C. The Ser631 residue is located in the extracellular mouth of the pore (Schönherr and Heinemann, 1996). The S631A mutation causes a large positive shift in the voltage-dependence of inactivation (Zou *et al.*, 1998) such that the resulting channels are essentially non-inactivating. Ser620 is located in the inner pore, and mutation to Thr or Cys largely removes inactivation (Ficker *et al.*, 1998). In contrast to the notion that inactivation plays a critical role in drug-mediated hERG blockade, fentanyl blocked S631A and S620C mutant hERG currents more potently than WT (Fig. 6), while S620T decreased the potency of hERG block by fentanyl. The IC_{50} values were 0.9±0.2 μM for WT (Hill coefficient: 1.1±0.2), 0.5±0.3 μM for S631A (Hill coefficient: 1.2±0.2), 0.05±0.07 μM for S620C (Hill coefficient: 0.6±0.2), and 3.5±1.4 μM for S620T (Hill coefficient: 1.1±0.2). In particular, although both S620T and S620C removed hERG inactivation, they displayed very different sensitivities to fentanyl. Thus,

Molecular Pharmacology Fast Forward. Published on January 21, 2019 as DOI: 10.1124/mol.118.114751
This article has not been copyedited and formatted. The final version may differ from this version.

unlike other hERG blockers (Ficker *et al.*, 1998; Wang *et al.*, 1997; Zhang *et al.*, 1999; Chen *et al.*, 2002), inactivation does not play an important role in fentanyl-mediated block of hERG channels.

Fentanyl blocks hERG in a voltage-dependent manner

We measured tail currents upon −50 mV repolarization following a 4-s 50-mV depolarizing step for WT hERG channels, but pulse currents upon 50 mV depolarization for inactivation-deficient mutant hERG channels to construct concentration-response relationships. To investigate if hERG block by fentanyl is voltage-dependent, we used inactivation-deficient channels to analyze fentanyl-mediated block at various voltages without interference from inactivation. Specifically, we used S631A and S620T mutant channels, as well as WT channels in the presence of 2 μM of ICA-105574 (3-nitro-N-(4-phenoxyphenyl) benzamide), which removes inactivation (Gerlach *et al.*, 2010).

First, we recorded currents by depolarizing steps to voltages from −70 to 70 mV in 10 mV increments followed by a repolarizing step to −50 mV in the absence and presence of fentanyl (Fig. 7). For S631A, S620T, and WT with ICA-105574, 3, 30, or 2 μM fentanyl was applied respectively in order to achieve a high degree of block while leaving some currents for analysis. The normalized pulse current - and tail current - voltage relationships were constructed in the absence (control, CTL) and presence of fentanyl. Two observations are immediately obvious: first, fentanyl reduced the pulse currents to a greater extent than the tail current. Second, fentanyl decreased pulse current more at higher voltages (Fig. 7).

The voltage-dependence of hERG channel block by fentanyl was examined further. From a holding potential of −80 mV, cells were depolarized to 50 mV for 4 s to activate channels. This

Molecular Pharmacology Fast Forward. Published on January 21, 2019 as DOI: 10.1124/mol.118.114751
This article has not been copyedited and formatted. The final version may differ from this version.

was followed by test steps from 70 mV to −50 mV in 20 mV decrements for 5 s before returning to the holding potential (Fig. 8, top row). The current amplitudes after 100-ms of test steps were plotted against the voltages to construct normalized current-voltage relationships. While the current increased with voltage in control, it was bell-shaped in the presence of fentanyl (Fig. 8, middle row). When the ratio of current with fentanyl versus control was plotted against test voltage, it decreased linearly as voltage increased (Fig. 8, bottom row), demonstrating an increased block at higher voltages.

Fentanyl blocks I_{hERG} with a greater potency using an AP voltage protocol

Given the voltage-dependence of fentanyl-mediated block of hERG channels, we were interested in examining how it affects hERG current during cardiac AP voltages. To this end, we used a ventricular AP voltage-clamp waveform to elicit I_{hERG} and examined the concentration-dependence of fentanyl block. Fentanyl blocked I_{hERG} with an IC_{50} of 0.3±0.1 μM and a Hill coefficient of 0.9±0.1 (Fig. 9).

Fentanyl decreases I_{Kr} and prolongs APs in neonatal rat ventricular myocytes

We examined the effects of fentanyl on the native I_{hERG} counterpart, I_{Kr}, as well as I_{Na} and I_{Ca} in isolated neonatal rat ventricular myocytes. To determine the effects of fentanyl on I_{Kr}, we recorded I_K with a voltage protocol that first involves 1-s stepwise depolarizations from −70 to 70 mV in 10 mV increments, followed by a 1-s step at −50 mV before returning to holding potential of −80 mV. As we previously demonstrated using this protocol, the tail current upon −50 mV primarily represents I_{Kr} (Guo *et al.*, 2007). Application of 0.5 μM fentanyl decreased tail current (Fig. 10A, $P<0.05$ at 10 mV and above versus control), with complete recovery upon

washout (Fig. 10A, P>0.05 versus control). The tail current indeed represents I_{Kr} as it was essentially abolished by 1 μM of the selective I_{Kr} blocker, E-4031 (Fig. 10A). On the other hand, fentanyl at a concentration of 10 μM did not affect I_{Na} or Ba^{2+}-mediated I_{Ca} ($I_{Ca\text{-}Ba}$) (P>0.05, compared to control) (Fig. 10 B&C).

Whole-cell current-clamp was used to record APs in isolated neonatal rat ventricular myocytes. Fentanyl (0.5 μM) prolonged AP duration at 90% repolarization (APD_{90}) compared to control, and this effect was reversed upon washout (Fig. 10D). The mean APD_{90} was 298.3±83.7 ms for control, 404.4±84.4 ms with fentanyl (P<0.01 versus control), and 269.7±71.7 ms upon washout (P>0.05 versus control).

DISCUSSION

Fentanyl-associated death represents a serious issue in North America. While fentanyl gives rise to respiratory depression (Santiago and Edelman, 1985), it also prolongs the AP in isolated canine cardiac Purkinje fibers (Blair *et al.*, 1989). In a previous study, Vormberge *et al.* found that droperidol-/fentanyl-/N_2O-anesthetized dogs display a higher sensitivity to sotalol-induced QT prolongation than conscious dogs (Vormberge *et al.*, 2006). By recording rabbit Purkinje fiber APs and I_{hERG} from hERG-HEK cells, the authors concluded that the higher sensitivity of anesthetized dogs towards sotalol-induced QT-prolongation is due to a reduced cardiac repolarization reserve caused by droperidol-mediated blockade of hERG channels. Thus, while both droperidol and fentanyl were used as anesthetics in this study, droperidol, but not fentanyl, was studied (Vormberge *et al.*, 2006). On the other hand, Katchman *et al*. described the effects of various opioid agonists including fentanyl, methadone, L-α-acetylmethadol, meperidine, codeine, morphine, and buprenorphine on I_{hERG} recorded from hERG-HEK cells

(Katchman *et al.*, 2002). While this study showed that fentanyl blocks I_{hERG} with an IC_{50} of 1.8 μM, and methadone blocks I_{hERG} in the closed and open/inactivated states, the mechanisms of fentanyl-hERG interaction, as well as the effects of fentanyl on native I_{Kr} and APs in cardiomyocytes were not investigated.

The present study represents the first systemic investigation of the effects of fentanyl on I_{hERG} in hERG-HEK cells and I_{Kr} in neonatal rat ventricular myocytes. Our results revealed that, in contrast to many hERG blockers such as dofetilide, whose high affinity binding require channel inactivation (Ficker *et al.*, 1998), fentanyl blocked hERG channels in the open state (Fig. 4), but inactivation gating did not play a role in the fentanyl-hERG interaction (Fig. 6). We also demonstrated that fentanyl decreased I_{Kr} and prolonged APD_{90} in neonatal rat ventricular myocytes (Fig. 10).

Regarding the molecular mechanisms that underlie fentanyl-mediated hERG block, our study revealed that while fentanyl shares some properties with other hERG blockers, it possesses several novel properties. Previous mutagenesis and electrophysiological assays have shown that residues Thr623 and Val625 of the pore helix, and Gly648, Tyr652, and Phe656 of the S6 transmembrane segment are crucial for high-affinity binding of various compounds (Mitcheson *et al.*, 2000a). Although we did not examine Thr623, Val625, or Gly648 mutations, we did show that Y652A and F656T mutant hERG channels are resistant to block by fentanyl (Fig. 5B). Furthermore, we found that fentanyl competed with E-4031 for binding to hERG (Fig. 5A). These data suggest that fentanyl occupies the common drug binding site within the internal pore-mouth of the hERG channel. We propose that fentanyl enters the binding site and interacts with residues that line hydrophobic pockets (Wang and MacKinnon, 2017). The aromatic side chain

of fentanyl may form π-stacking interactions with residues in the hydrophobic pockets including Tyr652 and Phe656, leading to a blockade of hERG current.

In support of this theory, norfentanyl, the main metabolite of fentanyl produced when the phenyl-containing side chain is removed through N-dealkylation by liver enzymes (Labroo *et al.*, 1997), does not block I_{hERG} (Fig. 1B). This is in contrast to O-demethylation of astemizole, as desmethylastemizole, the principle metabolite of astemizole, blocks hERG channels with a similar potency (Zhou *et al.*, 1999). However, N-dealkylation of astemizole, which removes a phenyl-containing side chain to create norastemizole (a secondary metabolite), decreases block potency (Zhou *et al.*, 1999). This indicates that side chains containing phenyl groups are important for hERG block by drugs like fentanyl and astemizole. Since fentanyl is primarily metabolized to norfentanyl (Labroo *et al.*, 1997), the difference in hERG blocking properties is of clinical significance. First, drugs or conditions that decrease liver enzyme activity would increase fentanyl concentration, increasing the risk of hERG block. Second, naloxone does not reverse the decrease in I_{hERG} by fentanyl (Fig. 1C). Increasing liver enzyme activity is a promising therapeutic intervention for fentanyl-induced hERG toxicity, where arrhythmias and sudden death represent a concern.

Inactivation plays a critical role in high-affinity hERG binding by many compounds such as dofetilide, verapamil, E-4031, and cisapride (Ficker *et al.*, 1998; Zhang *et al.*, 1999; Chen *et al.*, 2002). Given that fentanyl appears to block hERG via targeting a typical binding site, it is interesting that unlike many compounds, inactivation does not play a role in hERG block by fentanyl (Fig. 6). The reason for this discrepancy is unknown but is likely related to the distinct tertiary structure of fentanyl, for which inactivation-induced conformational change of hERG is

not required for high-affinity binding. In this regard, we previously demonstrated that inactivation does not play a role in cocaine block of hERG channels (Guo *et al.*, 2006).

Our results showed that while S631A and S620C were blocked by fentanyl with a greater potency than WT channels, S620T displayed a reduced sensitivity (Fig. 6). S620T is consistently more resistant to block than other inactivation-deficient mutants (Ficker *et al.*, 1998; Zhang *et al.*, 1999). Since Ser620 is within the inner pore of hERG (Chen *et al.*, 2002; Ficker *et al.*, 1998), it may be involved in drug interaction with the channel. While the Cys molecule, similar in size to the Ser residue in WT, conserves the high-affinity binding site, the larger Thr residue may disrupt it. In support of this theory, despite disrupting inactivation to the same extent, hERG channels with four S620T subunits are more resistant to cisapride, dofetilide, and MK-499 block than channels with one S620T subunit and three WT subunits (Wu *et al.*, 2015). Thus, we have dissociated inactivation from fentanyl block. However, channel opening is a prerequisite for fentanyl to block hERG channels as block does not develop until the channel is open (Fig. 4, top). Once open, the block clearly develops in the first trace after fentanyl application. A smaller current with decay was observed in subsequent traces. This very small decay is consistent with fentanyl being trapped with minimal unbinding when hERG is held in the closed state. Even after completely removing fentanyl from the bath solution, hERG current does not recover until the channels are opened (Fig. 4B).

Another interesting finding is the voltage-dependence of hERG block by fentanyl. Using hERG channels with inactivation removed by mutations or drug, our results demonstrated a nearly linear voltage-dependence of fentanyl block between −50 and 70 mV, with greater block at more positive voltages (Fig. 8). Like most hERG blockers such as verapamil (Zhang *et al.*, 1999), we propose that fentanyl enters the binding site within the pore from the internal side of

the membrane. Fentanyl has a pKa of 8.12, meaning it is mostly positively charged at physiological pH (Thurlkill *et al.*, 2005). Thus, positive voltages may repel the positively charged fentanyl molecule deeper into the internal pore mouth. Upon discovering that fentanyl blocks hERG in a voltage-dependent manner, we investigated fentanyl block with a voltage protocol that mimics a cardiac AP. Interestingly, while the IC_{50} for fentanyl block determined by measuring the tail current at −50 mV following channel activation at 50 mV was 0.9 μM (Fig. 1), it was 0.3 μM when analyzed using the more physiologically relevant AP voltage protocol (Fig. 9). This difference in potency is primarily due to voltage-dependent block, as peak hERG current during the AP protocol occurs at voltages more positive than −50 mV. This finding is clinically important as the hERG blocking effects of fentanyl are 6-fold more potent than originally described by Katchman *et al.* (2002).

We have shown that fentanyl blocked I_{hERG} with an IC_{50} of 0.3 μM (Fig. 9), and it prolonged the cardiac AP at a concentration of 0.5 μM (Fig. 10D). A retrospective study based on 112 fentanyl-related deaths reported that the mean post-mortem blood levels in deaths attributed solely to fentanyl was 25 μg/L (74.3 nM), with a range of 3 μg/L (8.9 nM) to 383 μg/L (1.14 μM) (Martin *et al.*, 2006). While the IC_{50} for fentanyl to block hERG is higher than the mean post-mortem blood level, the upper ranges do overlap. However, as these concentrations are post-mortem, higher concentrations due to a large bolus dose of fentanyl cannot be ruled out. Therapeutic levels of fentanyl are complicated by tolerance with continued use. Hospital inpatients have demonstrated blood fentanyl concentrations up to 9.9 μg/L (29.42 nM) with chronic treatment (Thompson *et al.*, 2007). It has been reported that after intravenous dose in rats, concentrations of fentanyl in heart tissue are 2-3 times higher than plasma (Hug, Jr. and Murphy, 1981). Thus, fentanyl may induce torsadogenic risk by blocking hERG channels,

leading to sudden death, especially under circumstances described below. First, chronic fentanyl users may experience periods of hypoxia due to respiratory depression (Santiago and Edelman, 1985). Chronic hypoxia reduces mature hERG density and whole cell current (Lamothe *et al.*, 2017). Second, Solis *et al.* found that intravenous fentanyl causes a prolonged increase in temperature due to metabolic brain activation and skin vasoconstriction (Solis E Jr *et al.*, 2017). Hyperthermia in the presence of I_{Kr} block increases the transmural dispersion of APD (Burashnikov *et al.*, 2008), which indicates a higher risk for arrhythmia (Surawicz, 1996). Fentanyl-mediated hERG blockade was analyzed at room temperature (22°C) in the present study. While our analysis at physiological temperature (37°C) did not alter fentanyl blocking potency (data not shown), the effects of increased temperature on transmural dispersion in the presence of fentanyl should not be ruled out. Finally, hypokalemia is associated with an impairment of hERG function (Guo *et al.*, 2009; Massaeli *et al.*, 2010). Therefore, arrhythmia risk may be increased when fentanyl is used by those with existing electrolyte imbalances or when used concomitantly with other medications that interfere with hERG function.

In summary, we presented fentanyl as a hERG channel blocker that was capable of prolonging APD_{90}. We also demonstrated that fentanyl blocked hERG current in concentration-, channel state-, and voltage-dependent manners, while inactivation did not play a role. Although this study does not conclusively demonstrate that hERG block by fentanyl is responsible for fentanyl-related death, it does provide an alternative molecular mechanism, especially for those with overdoses or circumstances where hERG function is compromised (e.g. hypoxia, hypokalemia, other drugs).

Conflict of Interest: The authors declare that they have no conflicts of interest with the contents of this article.

Authorship Contributions:

Participated in research design: Tschirhart and Zhang

Conducted experiments: Tschirhart, Li, and Guo

Performed data analysis: Tschirhart, Li, Guo, and Zhang

Wrote or contributed to the writing of the manuscript: Tschirhart and Zhang

References

Blair JR, Pruett J K, Introna R P, Adams R J and Balser J S (1989) Cardiac Electrophysiologic Effects of Fentanyl and Sufentanil in Canine Cardiac Purkinje Fibers. *Anesthesiology* **71**:565-570.

Burashnikov A, Shimizu W and Antzelevitch C (2008) Fever Accentuates Transmural Dispersion of Repolarization and Facilitates Development of Early Afterdepolarizations and Torsade De Pointes Under Long-QT Conditions. *Circ Arrhythm Electrophysiol* **1**:202-208.

Cafiero T, Di Minno R M and Di Iorio C (2011) QT Interval and QT Dispersion During the Induction of Anesthesia and Tracheal Intubation: a Comparison of Remifentanil and Fentanyl. *Minerva Anestesiol* **77**:160-165.

Chen J, Seebohm G and Sanguinetti M C (2002) Position of Aromatic Residues in the S6 Domain, Not Inactivation, Dictates Cisapride Sensitivity of HERG and Eag Potassium Channels. *Proc Natl Acad Sci U S A* **99**:12461-12466.

Curran ME, Splawski I, Timothy K W, Vincent G M, Green E D and Keating M T (1995) A Molecular Basis for Cardiac Arrhythmia: *HERG* Mutations Cause Long QT Syndrome. *Cell* **80**:795-803.

Fenichel RR, Malik M, Antzelevitch C, Sanguinetti M, Roden D M, Priori S G, Ruskin J N, Lipicky R J and Cantilena L R (2004) Drug-Induced Torsades De Pointes and Implications for Drug Development. *J Cardiovasc Electrophysiol* **15**:475-495.

Ficker E, Jarolimek W, Kiehn J, Baumann A and Brown A M (1998) Molecular Determinants of Dofetilide Block of HERG K^+ Channels. *Circ Res* **82**:386-395.

Gerlach AC, Stoehr S J and Castle N A (2010) Pharmacological Removal of Human Ether-a-Go-Go-Related Gene Potassium Channel Inactivation by 3-Nitro-N-(4-Phenoxyphenyl) Benzamide (ICA-105574). *Mol Pharmacol* **77**:58-68.

Guo J, Gang H and Zhang S (2006) Molecular Determinants of Cocaine Block of HERG Potassium Channels. *J Pharmacol Exp Ther* **317**:865-874.

Guo J, Massaeli H, Li W, Xu J, Luo T, Shaw J, Kirshenbaum L A and Zhang S (2007) Identification of I_{Kr} and Its Trafficking Disruption Induced by Probucol in Cultured Neonatal Rat Cardiomyocytes. *J Pharmacol Exp Ther* **321**:911-920.

Guo J, Massaeli H, Xu J, Jia Z, Wigle J T, Mesaeli N and Zhang S (2009) Extracellular K^+ Concentration Controls Cell Surface Density of I_{Kr} in Rabbit Hearts and of the HERG Channel in Human Cell Lines. *J Clin Invest* **119**:2745-2757.

Hug CC, Jr. and Murphy M R (1981) Tissue Redistribution of Fentanyl and Termination of Its Effects in Rats. *Anesthesiology* **55**:369-375.

Katchman AN, McGroary K A, Kilborn M J, Kornick C A, Manfredi P L, Woosley R L and Ebert S N (2002) Influence of Opioid Agonists on Cardiac Human Ether-a-Go-Go-Related Gene K^+ Currents. *J Pharmacol Exp Ther* **303**:688-694.

Keating MT and Sanguinetti M C (2001) Molecular and Cellular Mechanisms of Cardiac Arrhythmias. *Cell* **104**:569-580.

Keller GA, Alvarez P A, Ponte M L, Belloso W H, Bagnes C, Sparanochia C, Gonzalez C D, Villa Etchegoyen M C, Diez R A and Di Girolamo G (2016) Drug-Induced QTc Interval Prolongation: A Multicenter Study to Detect Drugs and Clinical Factors Involved in Every Day Practice. *Curr Drug Saf* **11**:86-98.

Kornick CA, Kilborn M J, Santiago-Palma J, Schulman G, Thaler H T, Keefe D L, Katchman A N, Pezzullo J C, Ebert S N, Woosley R L, Payne R and Manfredi P L (2003) QTc Interval Prolongation Associated With Intravenous Methadone. *Pain* **105**:499-506.

Krantz MJ, Kutinsky I B, Robertson A D and Mehler P S (2003) Dose-Related Effects of Methadone on QT Prolongation in a Series of Patients With Torsade De Pointes. *Pharmacotherapy* **23**:802-805.

Labroo RB, Paine M F, Thummel K E and Kharasch E D (1997) Fentanyl Metabolism by Human Hepatic and Intestinal Cytochrome P450 3A4: Implications for Interindividual Variability in Disposition, Efficacy, and Drug Interactions. *Drug Metab Dispos* **25**:1072-1080.

Lamothe SM, Song W, Guo J, Li W, Yang T, Baranchuk A, Graham C H and Zhang S (2017) Hypoxia Reduces Mature HERG Channels Through Calpain Up-Regulation. *FASEB J* **31**:5068-5077.

Lees-Miller JP, Duan Y, Teng G Q and Duff H J (2000) Molecular Determinant of High-Affinity Dofetilide Binding to HERG1 Expressed in Xenopus Oocytes: Involvement of S6 Sites. *Mol Pharmacol* **57**:367-374.

Maremmani I, Pacini M, Cesaroni C, Lovrecic M, Perugi G and Tagliamonte A (2005) QTc Interval Prolongation in Patients on Long-Term Methadone Maintenance Therapy. *Eur Addict Res* **11**:44-49.

Martell BA, Arnsten J H, Krantz M J and Gourevitch M N (2005) Impact of Methadone Treatment on Cardiac Repolarization and Conduction in Opioid Users. *Am J Cardiol* **95**:915-918.

Martin TL, Woodall K L and McLellan B A (2006) Fentanyl-Related Deaths in Ontario, Canada: Toxicological Findings and Circumstances of Death in 112 Cases (2002-2004). *J Anal Toxicol* **30**:603-610.

Massaeli H, Guo J, Xu J and Zhang S (2010) Extracellular K^+ Is a Prerequisite for the Function and Plasma Membrane Stability of HERG Channels. *Circ Res* **106**:1072-1082.

Mitcheson JS, Chen J, Lin M, Culberson C and Sanguinetti M C (2000a) A Structural Basis for Drug-Induced Long QT Syndrome. *Proc Natl Acad Sci U S A* **97**:12329-12333.

Mitcheson JS, Chen J and Sanguinetti M C (2000b) Trapping of a Methanesulfonanilide by Closure of the HERG Potassium Channel Activation Gate. *J Gen Physiol* **115**:229-240.

Perry M, de Groot M J, Helliwell R, Leishman D, Tristani-Firouzi M, Sanguinetti M C and Mitcheson J (2004) Structural Determinants of HERG Channel Block by Clofilium and Ibutilide. *Mol Pharmacol* **66**:240-249.

Raynor K, Kong H, Chen Y, Yasuda K, Yu L, Bell G I and Reisine T (1994) Pharmacological Characterization of the Cloned Kappa-, Delta-, and Mu-Opioid Receptors. *Mol Pharmacol* **45**:330-334.

Sanguinetti MC, Jiang C, Curran M E and Keating M T (1995) A Mechanistic Link Between an Inherited and an Acquired Cardiac Arrhythmia: *HERG* Encodes the I_{Kr} Potassium Channel. *Cell* **81**:299-307.

Sanguinetti MC and Jurkiewicz N K (1990) Two Components of Delayed Rectifier K^+ Current: Differential Sensitivity to Black by Class III Antiarrhythmic Agents. *J Gen Physiol* **96**:195-215.

Santiago TV and Edelman N H (1985) Opioids and Breathing. *J Appl Physiol (1985)* **59**:1675-1685.

Schönherr R and Heinemann S H (1996) Molecular Determinants for Activation and Inactivation of HERG, a Human Inward Rectifier Potassium Channel. *J Physiol (Camb)* **493**:635-642.

Solis E Jr, Cameron-Burr K T and Kiyatkin E A (2017) Heroin Contaminated With Fentanyl Dramatically Enhances Brain Hypoxia and Induces Brain Hypothermia. *eNeuro* **4**.

Spector PS, Curran M E, Keating M T and Sanguinetti M C (1996a) Class III Antiarrhythmic Drugs Block HERG, a Human Cardiac Delayed Rectifier K^+ Channel - Open-Channel Block by Methanesulfonanilides. *Circ Res* **78**:499-503.

Spector PS, Curran M E, Zou A R and Sanguinetti M C (1996b) Fast Inactivation Causes Rectification of the I_{Kr} Channel. *J Gen Physiol* **107**:611-619.

Stanley TH (2014) The Fentanyl Story. *J Pain* **15**:1215-1226.

Stork D, Timin E N, Berjukow S, Huber C, Hohaus A, Auer M and Hering S (2007) State Dependent Dissociation of HERG Channel Inhibitors. *Br J Pharmacol* **151**:1368-1376.

Surawicz B (1996) Will QT Dispersion Play a Role in Clinical Decision-Making? *J Cardiovasc Electrophysiol* **7**:777-784.

Thompson JG, Baker A M, Bracey A H, Seningen J, Kloss J S, Strobl A Q and Apple F S (2007) Fentanyl Concentrations in 23 Postmortem Cases From the Hennepin County Medical Examiner's Office. *J Forensic Sci* **52**:978-981.

Thurlkill RL, Cross D A, Scholtz J M and Pace C N (2005) PKa of Fentanyl Varies With Temperature: Implications for Acid-Base Management During Extremes of Body Temperature. *J Cardiothorac Vasc Anesth* **19**:759-762.

Trudeau MC, Warmke J W, Ganetzky B and Robertson G A (1995) HERG, a Human Inward Rectifier in the Voltage-Gated Potassium Channel Family. *Science* **269**:92-95.

Vormberge T, Hoffmann M and Himmel H (2006) Safety Pharmacology Assessment of Drug-Induced QT-Prolongation in Dogs With Reduced Repolarization Reserve. *J Pharmacol Toxicol Methods* **54**:130-140.

Wang D, Sun X and Sadee W (2007) Different Effects of Opioid Antagonists on Mu-, Delta-, and Kappa-Opioid Receptors With and Without Agonist Pretreatment. *J Pharmacol Exp Ther* **321**:544-552.

Wang S, Morales M J, Liu S, Strauss H C and Rasmusson R L (1997) Modulation of HERG Affinity for E-4031 by K^+_o and C-Type Inactivation. *FEBS Lett* **417**:43-47.

Wang W and MacKinnon R (2017) Cryo-EM Structure of the Open Human Ether-a-Go-Go-Related K^+ Channel HERG. *Cell* **169**:422-430.

Witchel HJ, Dempsey C E, Sessions R B, Perry M, Milnes J T, Hancox J C and Mitcheson J S (2004) The Low-Potency, Voltage-Dependent HERG Blocker Propafenone - Molecular Determinants and Drug Trapping. *Mol Pharmacol* **66**:1201-1212.

Wu W, Gardner A and Sanguinetti M C (2015) The Link Between Inactivation and High-Affinity Block of HERG1 Channels. *Mol Pharmacol* **87**:1042-1050.

Zhang S, Zhou Z, Gong Q, Makielski J C and January C T (1999) Mechanism of Block and Identification of the Verapamil Binding Domain to HERG Potassium Channels. *Circ Res* **84**:989-998.

Zhou Z, Gong Q, Epstein M L and January C T (1998a) HERG Channel Dysfunction in Human Long QT Syndrome. Intracellular Transport and Functional Defects. *J Biol Chem* **273**:21061-21066.

Zhou Z, Gong Q, Ye B, Fan Z, Makielski J C, Robertson G A and January C T (1998b) Properties of HERG Channels Stably Expressed in HEK 293 Cells Studied at Physiological Temperature. *Biophys J* **74**:230-241.

Zhou Z, Vorperian V R, Gong Q, Zhang S and January C T (1999) Block of HERG Potassium Channels by the Antihistamine Astemizole and Its Metabolites Desmethylastemizole and Norastemizole. *J Cardiovasc Electrophysiol* **10**:836-843.

Zou A, Xu Q P and Sanguinetti M C (1998) A Mutation in the Pore Region of HERG K^+ Channels Expressed in *Xenopus* Oocytes Reduces Rectification by Shifting the Voltage Dependence of Inactivation. *J Physiol (Camb)* **509**:129-137.

FOOTNOTES

This work was supported by the Canadian Institutes of Health Research [MOP 72911] and the

Heart and Stroke Foundation of Canada [G-17-0018754] to S. Z.

Molecular Pharmacology Fast Forward. Published on January 21, 2019 as DOI: 10.1124/mol.118.114751
This article has not been copyedited and formatted. The final version may differ from this version.

LEGENDS FOR FIGURES

Fig. 1. Fentanyl acutely blocks I_{hERG} but does not decrease hERG protein expression. (A) Representative hERG currents elicited using the voltage protocol above in control (CTL), and with 1 or 10 μM fentanyl. (B) Concentration-dependent effects of fentanyl (FENT), Naloxone (NAL), and Norfentanyl (NOR-FENT) on I_{hERG}. The numbers above the data points indicate the number of cells examined from 4 independent experiments. Error bars represent SD. (C) Box plots of I_{hERG} recorded from control (CTL), in the presence of fentanyl (1 μM, FENT), or fentanyl (1 μM) plus naloxone (10 μM, FENT+NAL) (n=12, $^{**}P<0.01$ *vs*. CTL). There is no significant difference (NS) in I_{hERG} between FENT and FENT+NAL. (D) Western blot analysis of effects of 16-h treatment with fentanyl, norfentanyl, or naloxone (10 μM, respectively) on hERG expression. Actin is used as a loading control. The intensity of each hERG upper band was normalized to the actin and then to the control in each gel, and summarized (n=5, $P>0.05$).

Fig. 2. Fentanyl selectively blocks hERG channels. Various currents elicited using the voltage protocol shown above in the absence (control, CTL) or presence of 10 μM of fentanyl are shown (upper). Peak tail currents for hERG, pulse currents at the end of the depolarizing step for EAG, Kv1.5, and KCNQ+KCNE1, peak currents during the depolarizing step for Kv4.3, and inward currents at the end of the hyperpolarizing step for Kir2.3 were used for analyzing current amplitudes. Current amplitudes with fentanyl were normalized to their respective controls and summarized. $^{**}P<0.01$ *vs*. CTL.

Fig. 3. Effects of fentanyl on hERG biophysical properties. (A) Voltage protocol, representative current traces, and summarized pulse and tail currents upon each depolarizing voltage in the absence (CTL, control) or presence of 1 μM fentanyl are shown. The pulse current

Molecular Pharmacology Fast Forward. Published on January 21, 2019 as DOI: 10.1124/mol.118.114751
This article has not been copyedited and formatted. The final version may differ from this version.

– voltage relationships were constructed by normalizing currents at the end of the depolarizing steps in the absence and presence of fentanyl to the maximal pulse current in control for each cell, and summarized against depolarizing voltages. The tail current – voltage relationships were constructed by normalizing the tail currents in the absence and presence of fentanyl to the maximal tail current in control for each cell, and summarized against depolarizing voltages (n=12). (B) Voltage protocol, representative currents (five traces shown for clarity), and τ_{inact} at corresponding voltages are shown (n=4). (C) Voltage protocol, representative currents (four traces shown for clarity), and τ_{recv} at corresponding test voltages are shown (n=5). (D) Fast ($\tau_{f\text{-}deact}$) and slow ($\tau_{s\text{-}deact}$) times constants of deactivating currents against test voltages exemplified in C are shown (n=5). Error bars represent SD.

Fig. 4. Fentanyl is an open channel blocker of hERG. (A) hERG currents in control (CTL) and the first three traces in the presence of 2 μM fentanyl (FENT) recorded with the voltage protocol shown above. The first trace with fentanyl is indicated by arrow a, and subsequent traces by arrow b. The pulse interval was 60 s, and fentanyl was immediately washed-in after the control current was recorded. (B) hERG current with fentanyl (FENT) and the first two traces after a complete washout of fentanyl (WASH). The first trace after fentanyl washout is indicated by arrow a, and subsequent trace by arrow b. The pulse interval was 60 s, and fentanyl was immediately washed-out after the current with fentanyl was recorded.

Fig. 5. Fentanyl competes with E-4031 for binding to hERG channels. (A) Blockade and washout of I_{hERG} by fentanyl, E-4031 and fentanyl plus E-4031. Left: I_{hERG} was instantly blocked by 10 μM fentanyl, and largely recovered within 1 min upon fentanyl washout (n=4). Middle:

Molecular Pharmacology Fast Forward. Published on January 21, 2019 as DOI: 10.1124/mol.118.114751
This article has not been copyedited and formatted. The final version may differ from this version.

I_{hERG} was blocked by 0.5 μM E-4031, and minimally recovered upon E-4031 washout (n=4). Right: Presence of fentanyl promoted I_{hERG} recovery upon E-4031 washout (n=7). (B) The Y652A or F656T mutation decreases fentanyl-mediated block of I_{hERG}. While 10 μM fentanyl nearly abolished WT I_{hERG}, it affected neither Y652A nor F656T I_{hERG}. The voltage protocol is the same as Fig. 3A. Peak tail currents upon the −50 mV step after 50 mV depolarization were used for current amplitude analysis. The current with fentanyl was normalized to the control current in the same cell, and plotted in each group. $^{**}P<0.01$ versus WT.

Fig. 6. Inactivation does not play a role in fentanyl mediated block of hERG channels. WT, S631A, S620T, or S620C hERG currents in the absence (control, CTL) or presence of fentanyl at various concentrations were elicited using the voltage protocol shown in Fig. 1A. Tail currents upon −50 mV after the 50 mV depolarizing pulse were used for analysis of WT channels, and current amplitudes at the end of the 50 mV depolarizing pulse were used for analysis of inactivation deficient mutant channels. Current amplitudes with fentanyl were normalized to control and plotted against drug concentrations. Data were fitted to the Hill equation to obtain IC_{50} values. Error bars represent SD. WT, n=5; S631A, n=3-15; S620T, n=5-8; and S620C, n=4-8.

Fig. 7. Fentanyl blocks pulse currents more than tail currents of inactivation-deficient hERG channels. Representative currents recorded using the voltage protocol shown at the top are shown above the normalized pulse current- and tail current-voltage relationships. For normalization, pulse and tail currents in the absence and presence of fentanyl were normalized to their respective maximal currents in control for each cell, and plotted against the depolarizing

voltages. While fentanyl largely reduced the pulse currents at positive voltages, it moderately reduced tail currents of S631A (n=5), S620T channels (n=8) or WT hERG with ICA-105574 (n=5). Error bars represent SD.

Fig. 8. Voltage-dependence of fentanyl block of inactivation-deficient hERG channels. S631A, S620T, and WT with ICA-105574 currents recorded using the voltage protocol shown above in the absence (control, CTL) or presence of 3, 30 or 2 μM fentanyl (FENT), respectively. The normalized current-voltage relationships in control (CTL) and with fentanyl (FENT) are shown in the middle. The currents measured after 100-ms of the test voltages between −50 and 70 mV in control and with fentanyl were normalized to the maximal currents in control for each cell, and plotted against the test voltages. Summarized ratios of currents with fentanyl versus currents in control plotted against test voltages are shown in the bottom. n=5 for S631A, n=8 for S620T, and n=5 for WT with ICA-105574. Error bars represent SD.

Fig. 9. Effects of fentanyl on I_{hERG} elicited using a human ventricular action potential protocol. The human ventricular action potential waveform (top) was applied to hERG-HEK cells to elicit I_{hERG}. Representative currents in control (CTL), with 0.5 or 10 μM fentanyl are shown (middle). Peak hERG currents with various concentrations of fentanyl were normalized to the control current in each cell, and summarized against fentanyl concentrations. Data were fitted to the Hill equation. The numbers above the data points indicate the number of cells examined from 3 independent experiments. Error bars represent SD.

Fig. 10. Fentanyl decreased I_{Kr} and prolonged action potentials in neonatal rat ventricular myocytes. (A) Fentanyl-induced reduction of I_{Kr}. Representative I_K recorded from neonatal rat ventricular myocytes in control, with 0.5 μM fentanyl, upon washout, and with 1 μM E-4031 are shown above summarized I_K-voltage relationships from 6 cells. E-4031 was used to demonstrate that tail current of I_K represents I_{Kr}, as it was selectively abolished. Tail currents at various voltages and conditions were normalized to the maximal tail current (following 70 mV depolarizing step) in control for each cell, and data from 6 cells were summarized. **P*< 0.05 at 10 mV and above compared with CTL. (B) Representative I_{Na} in control and with 10 μM fentanyl along with the summarized I_{Na}-voltage relationships (n=7). (C) Representative $I_{Ca\text{-}Ba}$ in control and with 10 μM fentanyl along with $I_{Ca\text{-}Ba}$-voltage relationships (n=5). (D) Representative action potentials in control, with 10 μM fentanyl, and upon washout along with summarized APD_{90} (n=9 cells from 3 independent experiments, 42 action potentials for control and fentanyl, 22 action potentials for washout). ***P*< 0.01 versus control. Error bars represent SD.

Molecular Pharmacology Fast Forward. Published on January 21, 2019 as DOI: 10.1124/mol.118.114751
This article has not been copyedited and formatted. The final version may differ from this version.

FIGURE 1

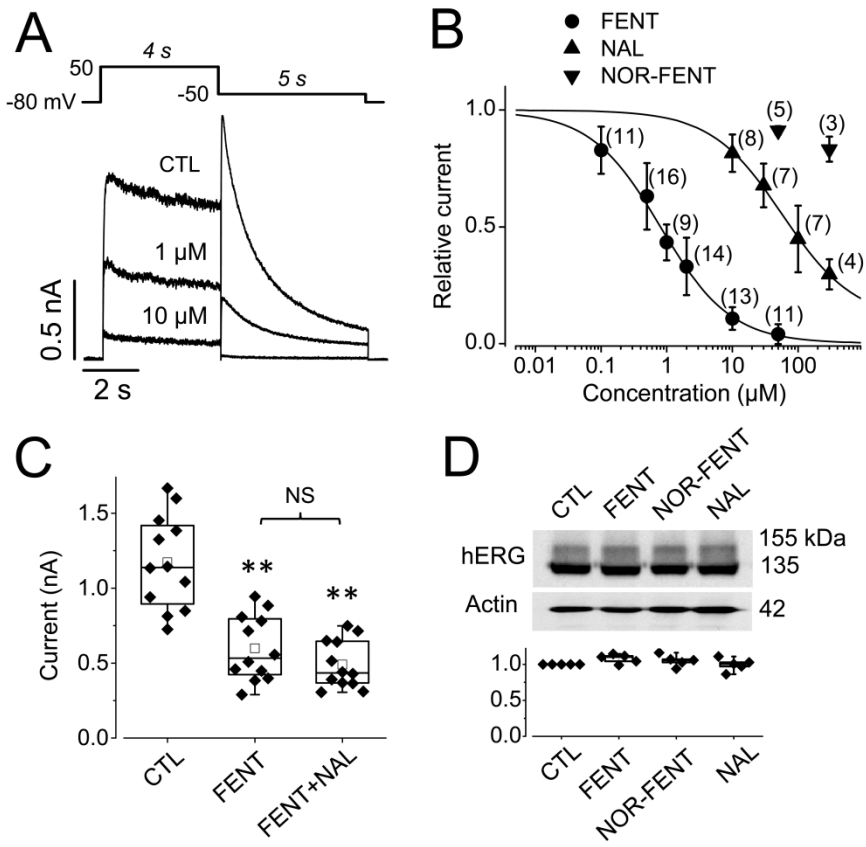

Molecular Pharmacology Fast Forward. Published on January 21, 2019 as DOI: 10.1124/mol.118.114751
This article has not been copyedited and formatted. The final version may differ from this version.

FIGURE 2

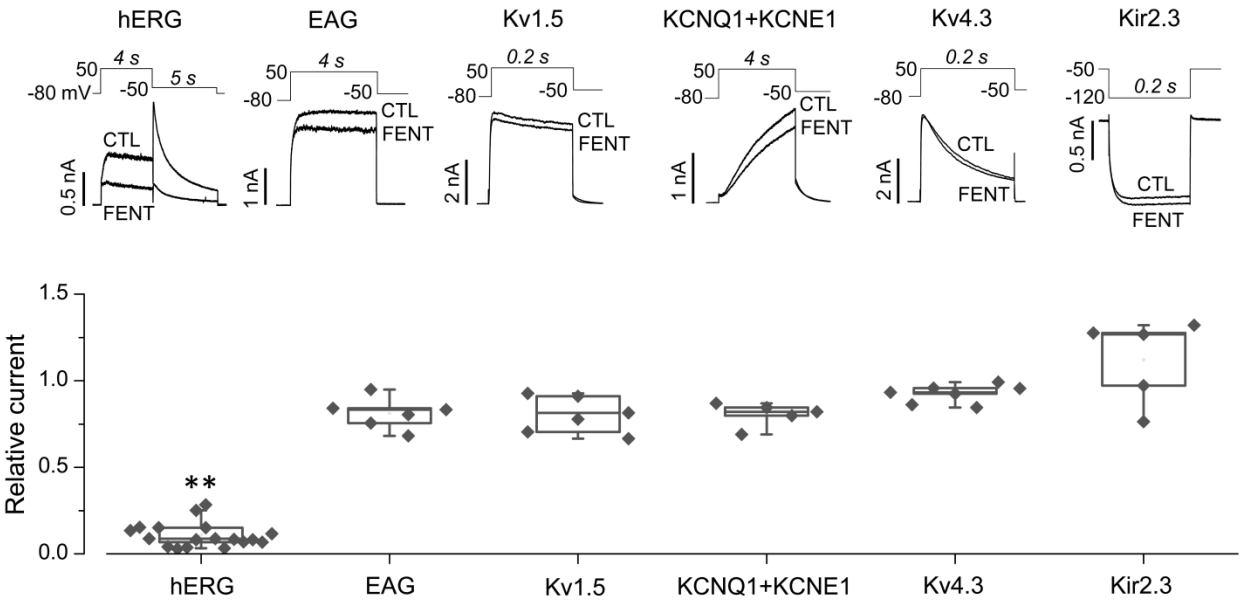

Molecular Pharmacology Fast Forward. Published on January 21, 2019 as DOI: 10.1124/mol.118.114751
This article has not been copyedited and formatted. The final version may differ from this version.

FIGURE 3

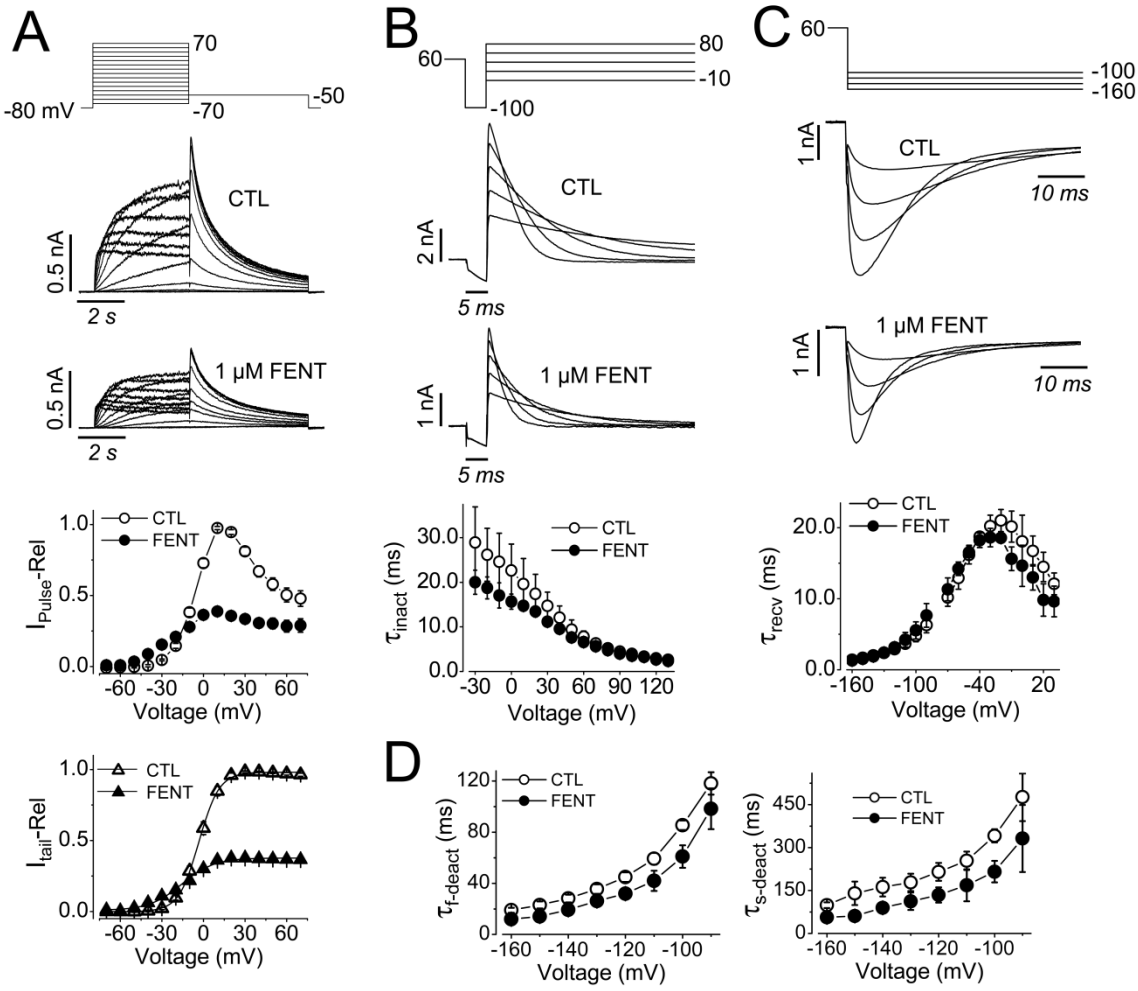

Molecular Pharmacology Fast Forward. Published on January 21, 2019 as DOI: 10.1124/mol.118.114751
This article has not been copyedited and formatted. The final version may differ from this version.

FIGURE 4

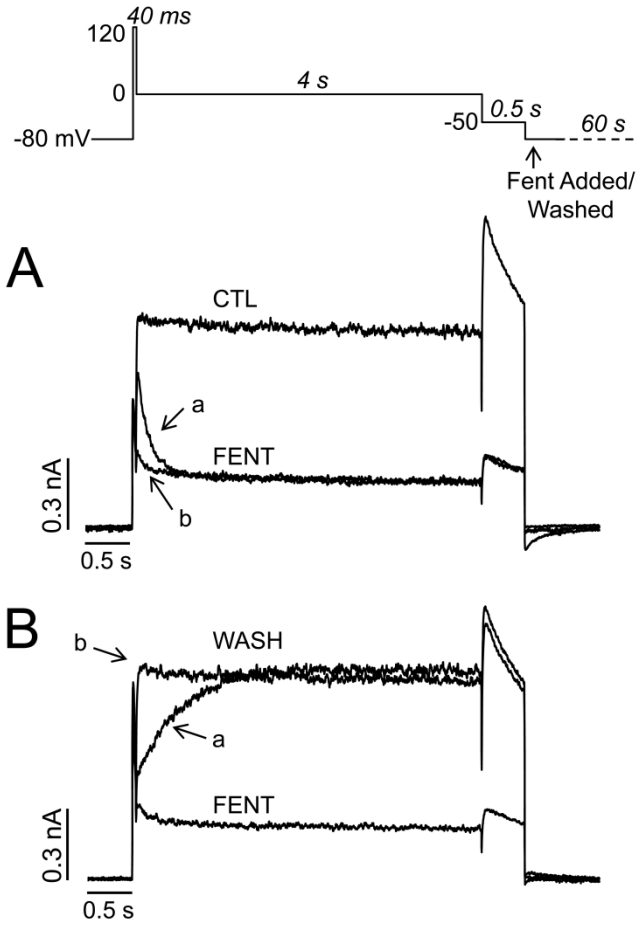

Molecular Pharmacology Fast Forward. Published on January 21, 2019 as DOI: 10.1124/mol.118.114751
This article has not been copyedited and formatted. The final version may differ from this version.

FIGURE 5

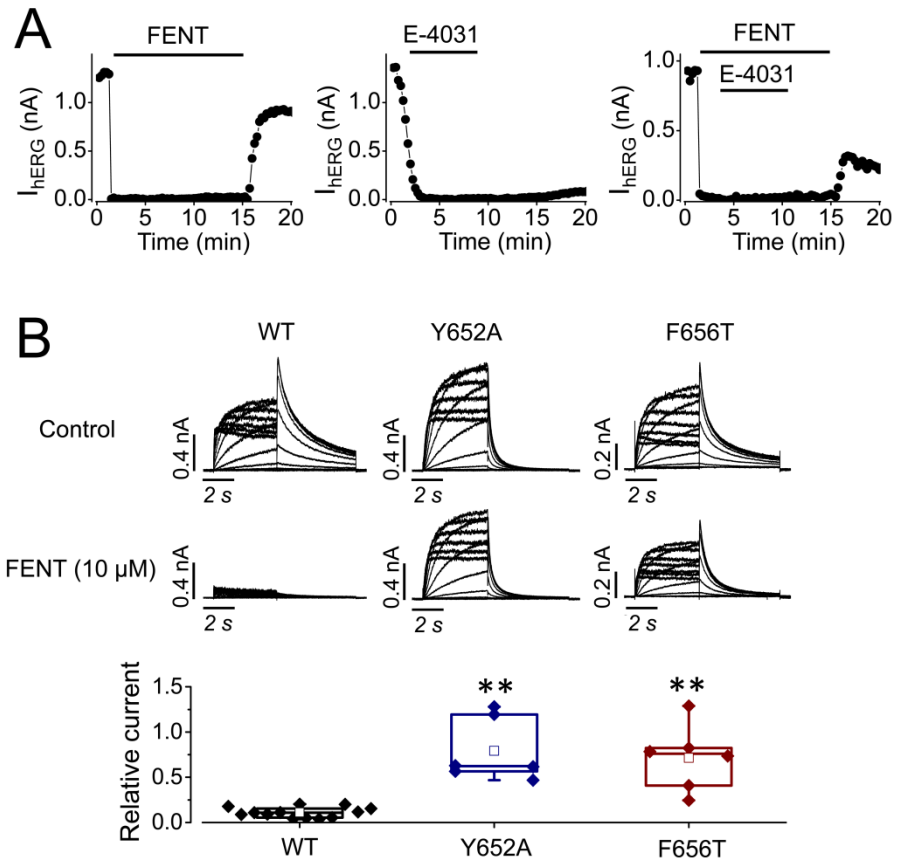

Molecular Pharmacology Fast Forward. Published on January 21, 2019 as DOI: 10.1124/mol.118.114751
This article has not been copyedited and formatted. The final version may differ from this version.

FIGURE 6

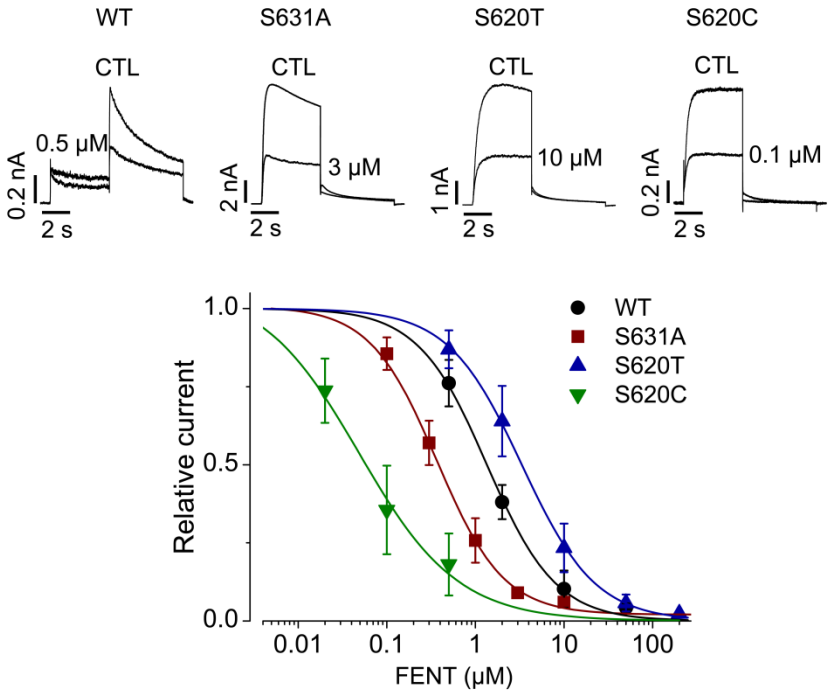

Molecular Pharmacology Fast Forward. Published on January 21, 2019 as DOI: 10.1124/mol.118.114751
This article has not been copyedited and formatted. The final version may differ from this version.

FIGURE 7

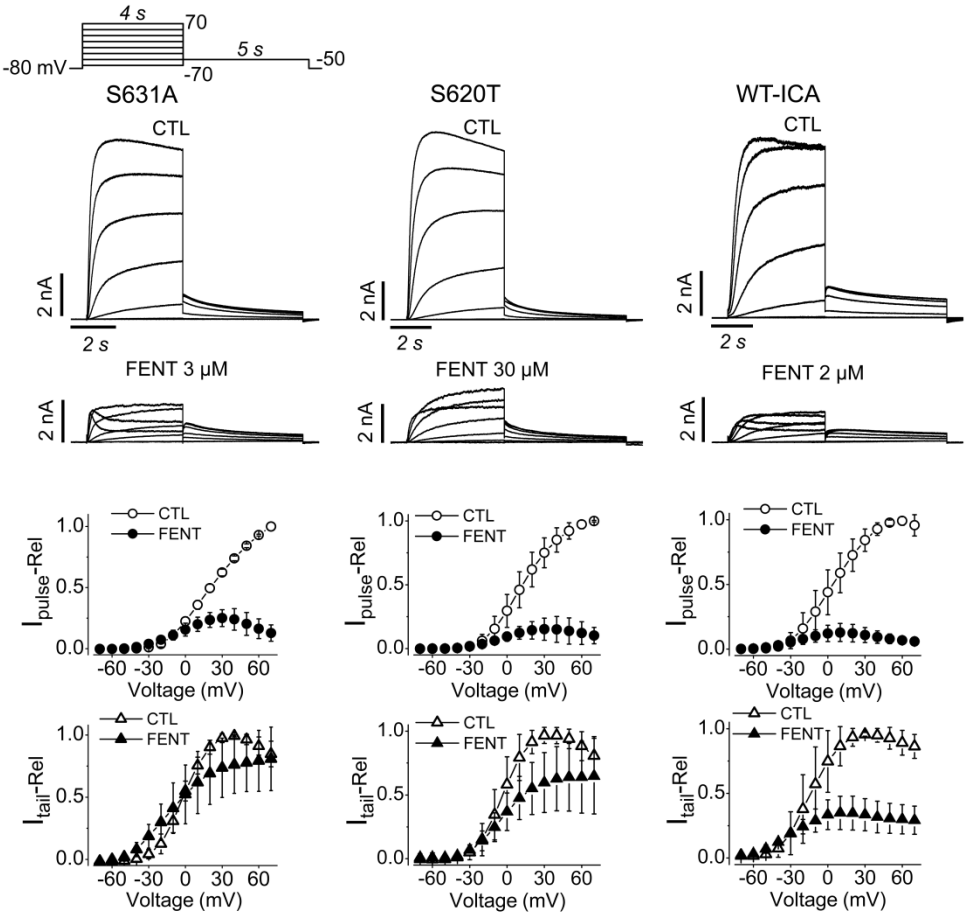

Molecular Pharmacology Fast Forward. Published on January 21, 2019 as DOI: 10.1124/mol.118.114751
This article has not been copyedited and formatted. The final version may differ from this version.

FIGURE 8

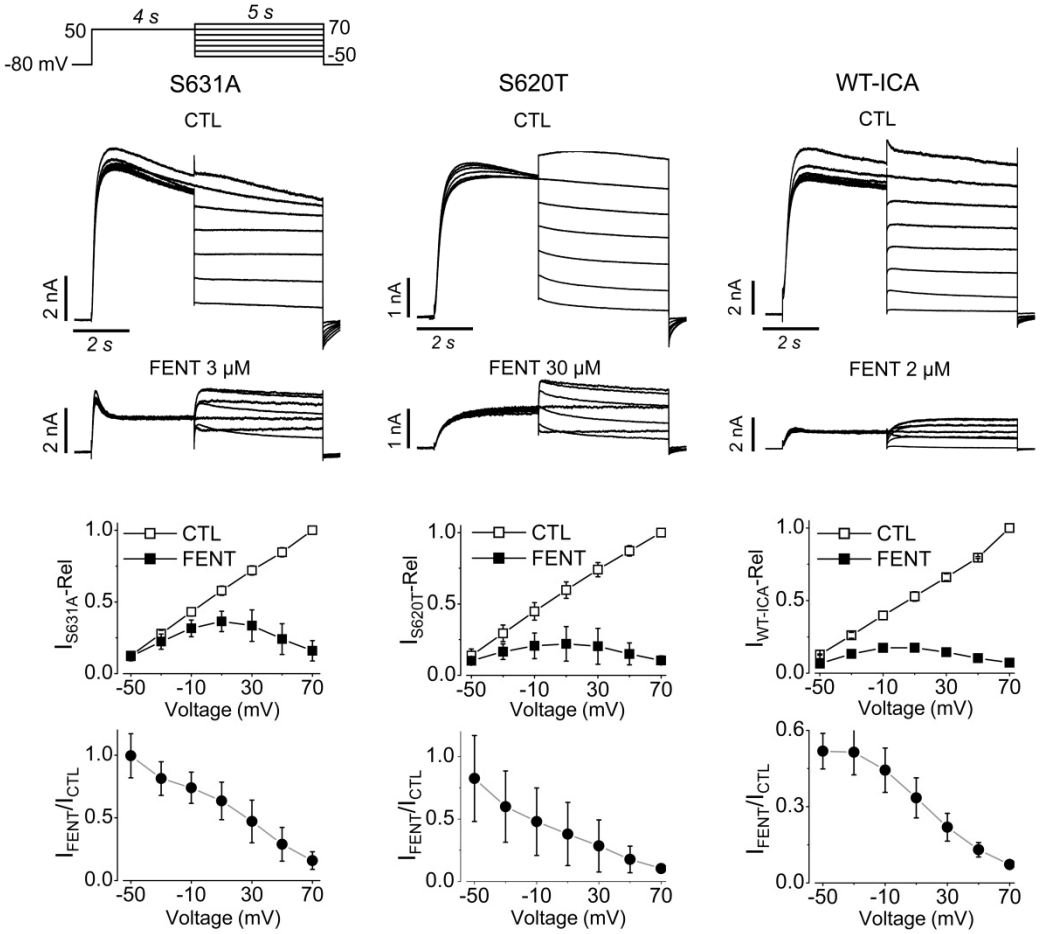

Molecular Pharmacology Fast Forward. Published on January 21, 2019 as DOI: 10.1124/mol.118.114751
This article has not been copyedited and formatted. The final version may differ from this version.

FIGURE 9

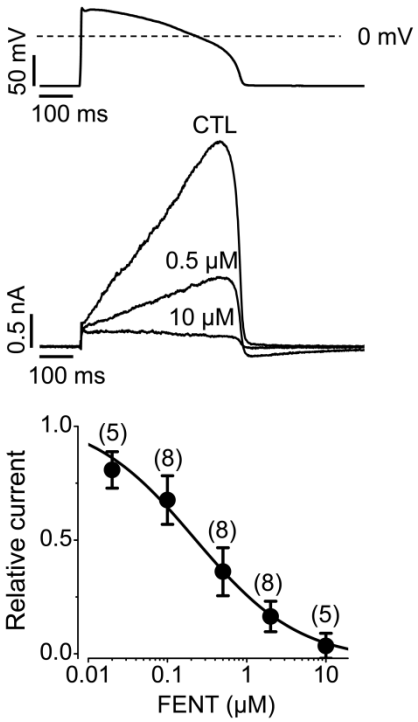

Molecular Pharmacology Fast Forward. Published on January 21, 2019 as DOI: 10.1124/mol.118.114751
This article has not been copyedited and formatted. The final version may differ from this version.

FIGURE 10